

A semi-microscopic approach to the backbending phenomena in even-even nuclei

This article has been downloaded from IOPscience. Please scroll down to see the full text article.

2013 J. Phys.: Conf. Ser. 413 012028

(<http://iopscience.iop.org/1742-6596/413/1/012028>)

View [the table of contents for this issue](#), or go to the [journal homepage](#) for more

Download details:

IP Address: 194.102.58.6

The article was downloaded on 28/02/2013 at 08:10

Please note that [terms and conditions apply](#).

A semi-microscopic approach to the backbending phenomena in even-even nuclei

A A Raduta^{1,2} and R Budaca¹

¹Horia Hulubei National Institute of Physics and Nuclear Engineering (IFIN-HH), PO Box MG-6, R-077125 Bucharest-Magurele, Romania

²Academy of Romanian Scientists, 54 Splaiul Independentei, Bucharest 050094, Romania

E-mail: raduta@nipne.ro

Abstract. The phenomenon of backbending in rare earth nuclei is described by means of the band hybridization mechanism. The hybridization of two rotational bands is performed by treating a model Hamiltonian associated with a set of interacting particles moving in a deformed mean field and coupled to a phenomenological core described in terms of quadrupole boson operators, in a product space of angular momentum projected states. The model states for the ground and S bands are obtained by angular momentum projection of a deformed product state with an axially symmetric coherent boson state standing for the core factor function and a BCS type single-particle factor function defining the nature of the band. The yrast band energies are defined by the lowest eigenvalues of the model Hamiltonian in an orthogonal basis constructed by diagonalizing the overlap matrix of the ground and S band states, which are not mutually orthogonal. The formalism is positively tested on six deformed even-even nuclei known to exhibit a backbending behavior in their moment of inertia.

1. Introduction

The backbending phenomenon is known to be the result of the crossing between the ground band and another band with a larger moment of inertia known as S (tockholm) band [1]. The S band is built on a broken pair with aligned individual high angular momentum. Such that in the rare earth region the first backbending is caused by the breaking of a neutron pair from the intruder orbital $i_{13/2}$, while the second one is due to the subsequent breaking of a proton $h_{11/2}$ pair. The first backbending is described in this work by means of a semi-microscopic model based on the bands hybridization mechanism. The physical system to be treated consists of a set of particles from the intruder orbital where the pair breaking occurs and a phenomenological deformed core defined by the remaining nucleons. The motion of the $i_{13/2}$ intruder neutrons is described by a BCS state, while the collective core by the Coherent State Model (CSM) [2]. The core deformation generates through the mutual coupling a deformed mean field for the single nucleon motion. However, the system is considered in the laboratory reference frame where the rotation invariance holds and thereby the angular momentum projected states should be constructed based on the intrinsic wave function defined above. Due to the deformation of the particle-core space the projected states are not mutually orthogonal. From this basis a new orthogonal basis is constructed which mixes the original projected states. The lowest eigenvalues of the model Hamiltonian in the orthogonal basis define the yrast band. Six even-even nuclei from the rare

earth region with $N = 90 - 94$, which exhibit a backbending behavior are quantitatively treated within the proposed formalism.

2. Theoretical framework

A particle-core Hamiltonian is treated in a space defined by a set of spherical projected product functions:

$$\Psi \equiv \psi_f \psi_c, \quad (1)$$

where ψ_f stands for the fermion factor state corresponding to the intruder particles and is chosen to be of BCS type, while the collective factor state ψ_c describing the core, is a coherent state for the quadrupole bosons b_{20}^\dagger :

$$\psi_c = e^{d(b_{20}^\dagger - b_{20})} |0\rangle_b. \quad (2)$$

$|0\rangle_b$ is the quadrupole boson vacuum state whereas d is a real parameter which actually simulates the nuclear deformation. The fermion factor function specifies the nature of the rotational band. Thus, the ground band (g band), where all neutrons are paired, is given by a deformed BCS state associated to the set of neutrons placed in the intruder deformed states. On the other hand, the S band, which crosses the g band and produces the backbending, is build upon a broken pair of particles whose states are no longer connected by a time reversal transformation. The time reversal symmetry breaking, in the present formalism, is achieved by applying the operator $J_+ \alpha_{jk}^\dagger \alpha_{j-k}^\dagger$ on the mentioned deformed BCS state with α_{jk}^\dagger being the creation operator for a quasiparticle in the single-particle state $|jk\rangle$.

The projected particle-core functions of the g and S band are obtained by applying the Hill-Wheeler projection operator on the product state (1) with a specific fermionic factor state and can be written in the following form:

$$\Psi_{JM}^{(1)} = \mathcal{N}_J^{(1)} P_{M0}^J |BCS\rangle_d \psi_c = \mathcal{N}_J^{(1)} \sum_{J_f J_c} \frac{C_{0\ 0\ 0}^{J_f J_c J}}{\mathcal{N}_{J_f}^{BCS} \mathcal{N}_{J_c}^{(g)}} \left[\Phi_{J_f}^{BCS} \phi_{J_c}^{(g)} \right]_{JM}, \quad (3)$$

$$\begin{aligned} \Psi_{JM;1}^{(2)}(jk) &= \mathcal{N}_{J1}^{(2)}(jk) P_{M1}^J \left[J_+ \alpha_{jk}^\dagger \alpha_{j-k}^\dagger |BCS\rangle_d \right] \psi_c \\ &= \mathcal{N}_{J1}^{(2)}(jk) \sum_{J_f J_c} \frac{C_{1\ 0\ 1}^{J_f J_c J}}{\mathcal{N}_{J_f 1}^{jk} \mathcal{N}_{J_c}^{(g)}} \left[\Phi_{J_f 1}^{jk} \phi_{J_c}^{(g)} \right]_{JM}, \end{aligned} \quad (4)$$

with the corresponding normalization factors

$$\left[\mathcal{N}_J^{(1)} \right]^{-2} = \sum_{J_f J_c} \left(\frac{C_{0\ 0\ 0}^{J_f J_c J}}{\mathcal{N}_{J_f}^{BCS} \mathcal{N}_{J_c}^{(g)}} \right)^2, \quad \left[\mathcal{N}_{J1}^{(2)}(jk) \right]^{-2} = \sum_{J_f J_c} \left(\frac{C_{1\ 0\ 1}^{J_f J_c J}}{\mathcal{N}_{J_f 1}^{jk} \mathcal{N}_{J_c}^{(g)}} \right)^2. \quad (5)$$

$\phi_{J_c}^{(g)}$ is the core projected state (2) with the norm equal to unity, while $\Phi_{J_f M_f}^{BCS}$ and $\Phi_{J_f 1; M_f}^{jk}$ from (3) and (4) are the angular momentum projected fermionic factor states corresponding to the $0qp$ and $2qp$ BCS states, respectively:

$$\Phi_{J_f M_f}^{BCS} = \mathcal{N}_{J_f}^{BCS} P_{M_f 0}^{J_f} |BCS\rangle_d, \quad \Phi_{J_f 1; M_f}^{jk} = \mathcal{N}_{J_f 1}^{jk} P_{M_f 1}^{J_f} J_+ \alpha_{jk}^\dagger \alpha_{j-k}^\dagger |BCS\rangle_d. \quad (6)$$

The norms of these states are calculated using the recipe given in Ref.[3], while the norm $\mathcal{N}_{J_c}^{(g)}$ of the projected coherent boson state (2) was presented by A. A. Raduta in Ref.[2] in connection to CSM. It is worth to mention that the summations from Eqs.(3) and (4) over J_f are restricted by $J_f \leq 24$. This upper limit value is provided by the group theory [4] and represents the maximal

angular momentum that can be realized in the $j = 13/2$ configuration, when the Pauli principle is obeyed.

The model Hamiltonian describing the particles and core interacting system is a sum of three terms:

$$H = H_c + H_p + H_{pc}. \quad (7)$$

The core Hamiltonian H_c is represented by the quadrupole boson number operator:

$$H_c = \hbar\omega_b \sum_{\mu} b_{2\mu}^{\dagger} b_{2\mu}, \quad (8)$$

while H_p is associated to a set of particles from an intruder shell model orbital j which interact between themselves through a pairing force:

$$H_p = (\varepsilon_{nlj} - \lambda) \sum_{m=all} c_{nljm}^{\dagger} c_{nljm} - \frac{G}{4} P_j^{\dagger} P_j, \quad (9)$$

where $P_j^{\dagger}(P_j)$ are creation(annihilation) operators of a Cooper pair in the intruder orbital j . The particles and core subsystems interact with each other by a quadrupole-quadrupole (qQ) and a spin-spin interaction

$$H_{pc} = H_{qQ} + H_C = -A_C \sum_{\mu, m, m'} \langle nljm | r^2 Y_{2\mu} | nljm' \rangle c_{nljm}^{\dagger} c_{nljm'} \left[b_{2-\mu}^{\dagger} (-)^{\mu} + b_{2\mu} \right] + C \vec{J}_c \cdot \vec{J}_f. \quad (10)$$

The particle-core interaction induces a mutual deformation for both the quadrupole bosons and the single-nucleon mean field. The later one can be written as

$$H_{mf} = \sum_{m=all} \varepsilon_{nljm} c_{nljm}^{\dagger} c_{nljm}, \quad (11)$$

with energies given in the first order of perturbation by:

$$\varepsilon_{nljm} = \varepsilon_{nlj} - 4dX_C(2n+3)C_{\frac{1}{2}0\frac{1}{2}}^{j2j} C_{m0m}^{j2j}, \quad \text{where } X_C = \frac{\hbar}{8M\omega_0} \sqrt{\frac{5}{\pi}} A_C. \quad (12)$$

Treating the sum $H_{mf} + H_{pair}$ through the BCS formalism, one obtains the occupation probabilities V and U , the energy gap Δ , the quasiparticle energies and the Fermi level energy, λ . With these quantities, the single-particle factor of the projected particle-core product basis is completely determined. Due to the dangerous graphs vanishing the matrix elements between total projected states of the single-particle term $H_{mf} + H_{pair}$ and of the qQ interaction, written in the quasiparticle representation, acquire very compact expressions due.

The matrix elements of the remaining Hamiltonian terms are easily obtained by using the tensorial form of the projected states (3) and (4). For the harmonic boson Hamiltonian we make use of its matrix elements on projected coherent states given in Ref.[5], while the spin-spin interaction matrix elements are obtained from the basic properties of the angular momentum operators. In this way the energy spectra of the g and S bands are completely determined by the average of the total Hamiltonian on the corresponding projected state, (3) or (4). In order to achieve the hybridization of these bands, one must diagonalize the total Hamiltonian in a basis defined by the projected states (3) and (4), which unfortunately are not orthogonal. However, using the eigenvalues $\alpha_m(J, jk)$ and the eigenvectors $V_{nm}(J, jk)$ of the overlap matrix defined by the non-orthogonal states, one can construct the functions [6]:

$$\Phi_m^{JM}(jk) = \frac{1}{\sqrt{\alpha_m(J, jk)}} \left[\Psi_{JM}^{(1)} V_{1m}(J, jk) + \Psi_{JM;1}^{(2)}(jk) V_{2m}(J, jk) \right], \quad m = 1, 2, \quad (13)$$

which are mutually orthogonal. Diagonalizing the total Hamiltonian in this orthogonal basis, for each angular momentum J one obtains a set of two hybridization energies, with the lowest ones defining the yrast band.

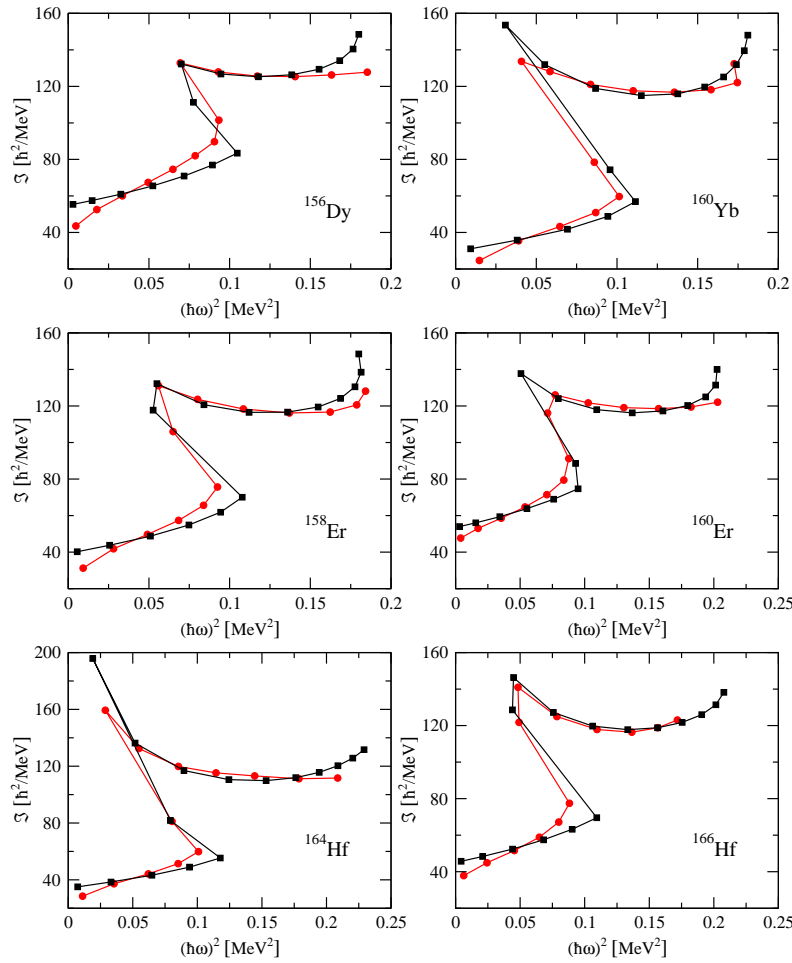


Figure 1. (color online) Backbending plots for ^{156}Dy , ^{160}Yb , $^{158,160}\text{Er}$ and $^{164,166}\text{Hf}$ isotopes comparing theory (black squares) with experiment (red circles). Experimental data are taken from [7, 8, 9, 10, 11].

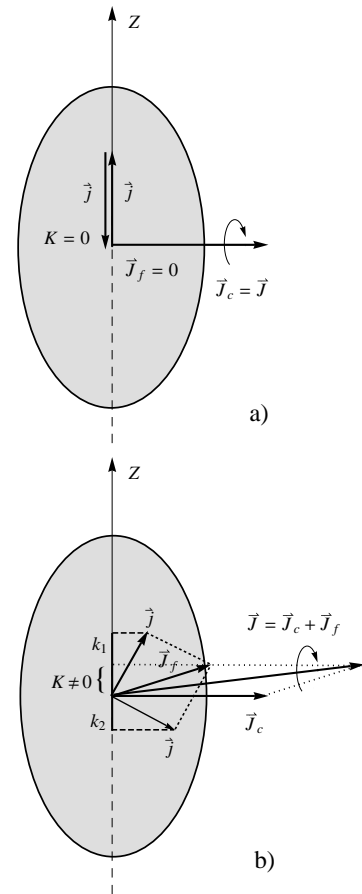


Figure 2. The coupling scheme for g band (a) and for S band (b).

3. Numerical application

The nuclei ^{156}Dy , ^{160}Yb , $^{158,160}\text{Er}$ and $^{164,166}\text{Hf}$ are known to be good backbenders. These nuclei are treated within the formalism described in the previous section. The model involves five free parameters, with four of them, namely, the pairing constant G , the qQ and spin-spin interaction strengths X_C and C , and the boson frequency $\hbar\omega_b$ being the structure coefficients of the model Hamiltonian. The remaining parameter is the deformation d which defines the collective factor state. The manner in which these parameters are fixed is detailed in Ref.[3]. Solving the BCS equations for an extended subset of 23 single-particle states comprising all possible levels which might interact with the $i_{13/2}$ intruder states, one obtains the gap parameter Δ , the Fermi level energy, the quasiparticle energies and consequently the occupation probabilities U and V . The input data for the BCS equations are the pairing constant G and the mean field single-particle energies defined by Eq.(12) and which depend linearly on the deformation parameter d . Collecting the BCS quantities only for the $i_{13/2}$ neutron orbital and using the values of the model parameters found in Ref.[3], one calculates the system energy by diagonalizing the total Hamiltonian in the orthogonal basis of states (13). The lowest hybridization energies for each angular momentum J defines the yrast band. It is worth mentioning that besides the

description of the energy spectra, the fitted parameters also reproduce the observed sequence of the single-particle levels with a deformation d being in the range of values determined in Refs.[12, 13].

The theoretical results are compared with experimental data in Fig.1 by means of backbending plots. The backbending plot is a graphical representation of the moment of inertia dependence on the angular frequency squared. From Fig.1 it is obvious that in all cases the general zigzag behavior is reproduced quite well. An especially good agreement is found for moderate spin states situated right in the backbending region. The theoretical yrast energies associated to the backbending plots from Fig.1 have the *r.m.s.* deviations of about 30 keV from the corresponding experimental energies. The angular momentum where the backbending starts represent the band crossing point. From Fig.1 one can see that for Er isotopes and ^{166}Hf the band crossing takes place at $J = 12$, while for ^{164}Hf and ^{160}Yb at $J = 10$, and for ^{156}Dy at $J = 14$. At the band crossing point there is a transition of the yrast band from $0qp$ to $2qp$ states caused by the breaking of a neutron intruder pair. The mechanism of pair breaking and the alignment of the involved angular momenta is visualized in Fig.2. At low values of the core angular momentum the nucleon angular momenta are anti-aligned along the symmetry axis of the mean-field ($\vec{J}_f = 0$) and the whole angular momentum is due to the core alone ($\vec{J}_c = \vec{J}$) which is perpendicular to the symmetry axis (Fig.2(a)). The alignment of the particle angular momenta to the core angular momentum is shown in Fig.2(b). The full alignment between the core and fermion angular momenta is not possible due to the fact that the total K for the two neutrons is equal to unity.

4. Conclusions

A semi-microscopic formalism was applied to describe the moment of inertia anomalies at low spins in even-even rare earth nuclei. The theoretical yrast energies obtained as the lowest eigenvalues of a particle-core Hamiltonian in an orthogonal basis constructed from the projected product states are used to calculate the backbending plots for six nuclei. The experimental backbending curves are fairly well reproduced by the numerical results of the proposed formalism. The shape and sharpness of the backbendings are in a good agreement with experiment. The first energy levels before the backbending are determined by the $0qp$ projected states and after a critical angular momentum, where the bands g and S cross each other, the states become of a $2qp$ nature. The advantage of the present formalism over other models consists in the fact that it also provides a qualitative explanation of the combined effect of the pair breaking mechanism and rotational alignment of the angular momenta implied in the system, on the backbending behavior of the moment of inertia. Concluding, one can say that the model proposed is able to describe quantitatively the main features of the first backbending in rare earth nuclei, revealing in the same time new features regarding its mechanism.

References

- [1] Johnson A, Reyde H and Sztarkier J 1971 *Phys. Lett. B* **34** 605
- [2] Raduta A A, Ceaurescu V, Gheorghe A and Dreizler R M 1982 *Nucl. Phys. A* **381** 253
- [3] Raduta A A and Budaca R 2012 *Phys. Rev. C* **84** 044323
- [4] Hamermesh N 1962 *Group Theory and its Application to Physical Problems* (New York: Dover Publications)
- [5] Raduta A A, Lo Iudice N and Ursu I I 1995 *Nucl. Phys. A* **584** 84
- [6] Raduta A A, Raduta C M and Faessler A 2009 *Phys. Rev. C* **80** 044327
- [7] Reich C W 2003 *Nucl. Data Sheets* **99** 753
- [8] Reich C W 1996 *Nucl. Data Sheets* **78** 547
- [9] Helmer R G 2004 *Nucl. Data Sheets* **101** 325
- [10] Balraj Singh 2001 *Nucl. Data Sheets* **93** 243
- [11] Shurshikov E N and Timofeeva N V 1992 *Nucl. Data Sheets* **67** 45
- [12] Raduta A A, Budaca R and Faessler A 2010 *J. Phys. G: Nucl. Part. Phys.* **37** 085108
- [13] Raduta A A, Budaca R and Faessler A 2012 *Ann. Phys. (NY)* **327** 671